Free-Standing Ordered Mesoporous Silica Films Synthesized with Surfactant−Polyelectrolyte Complexes at the Air/Water Interface

Bin Yang and Karen J. Edler*

Department of Chemistry, University of Bath, Claverton Down, Bath, Avon BA2 7AY, U.K.

Received July 29, 2008. Revised Manuscript Received January 26, 2009

Solid cetyltrimethylammonium bromide (CTAB) and polyethylenimine (PEI) films self-assemble at the air/water interface. Small angle X-ray scattering (SAXS) measurements show that dried films maintain the same ordered mesostructure as the films at the air/water interface, and here the effects of PEI concentration and cross-linker (CL) on film mesostructure were investigated. Free-standing silica films were then synthesized by adding tetramethoxysilane (TMOS) to the surfactant−polyelectrolyte solutions. Silica films have been studied by Brewster angle microscopy (BAM) and neutron reflectivity on as-synthesized films at the solution surface. Dried films have also been examined by SAXS and thermogravimetric analysis (TGA). On the basis of neutron reflectivity and SAXS data, a phase diagram for the CTAB−PEI−TMOS system has been drawn, and we propose a model for the formation of silica films synthesized with surfactant−polyelectrolyte complexes. The silica films retain their ordered mesostructure after surfactant removal, and polymer remains inside the silica wall when the surfactant has been washed out, which improves the mechanical properties of the films and may be used to add functionality to these membranes in future applications.

Introduction

Since scientists in Mobil reported highly ordered M41S mesoporous silicate molecular sieves templated by quaternary ammonium cationic surfactants,[1] materials with ordered mesopores and controllable structure have been extensively studied, as a result of their emerging applications in catalysis, adsorption, and separation. The "template" concept was postulated for the synthesis of mesoporous materials, in which the organic molecules and inorganic species cooperatively self-assemble into a mesostructured composite. Removal of the organic template results in mesoporous materials. Until now, most studies have focused on synthesis, formation mechanism, characterization, and modification of mesoporous powders; however, from the viewpoint of practical application, mesoporous materials with a film geometry have many advantages especially in chemical sensing, separation, and catalysis.

The most common ways to prepare inorganic films templated by surfactant from a precursor sol on a support are dip-coating,[2,3] spin coating,[4−7] and layer-by-layer strategies.[8,9] In dip and spin coating the micelles form and arrange on a substrate in an organized manner during evaporation of the solvent which induces the self-assembly of organic and inorganic species. Growing films from solution at an interface has also been studied. Yang et al. reported spontaneous formation of film on mica substrates,[10] while Schacht et al. showed the possibility of growing silica films at the oil−water interface.[11] In 1996, the spontaneous growth of free-standing mesostructured silica films at the air−solution interface was separately reported by Yang et al[12] and Aksay et al.[13] In these solutions inorganic and surfactant species interact forming larger liquid-like particles where microphase separation of the inorganic and surfactant under high concentration conditions results in the formation of the final 2D hexagonal mesostructure. These particles migrate to the interface to form the films.[14] Three dimensional hexagonal[15] and cubic[16] silica films were also prepared at the air−water interface. Compared to films grown by dip coating, spin coating, and the layer by layer method, the strategy of fabricating films at the air−solution interface,

(1) Kresge, C. T.; Leonowicz, M. E.; Roth, W. J.; Vartuli, J. C.; Beck, J. S. *Nature* **1992**, *359*, 710–712.
(2) Lu, Y. F.; Ganguli, R.; Drewien, C. A.; Anderson, M. T.; Brinker, C. J.; Gong, W. L.; Guo, Y. X.; Soyez, H.; Dunn, B.; Huang, M. H.; Zink, J. I. *Nature* **1997**, *389*, 364–368.
(3) Grosso, D.; Cagnol, F.; Soler-Illia, G. J. d. A. A.; Crepaldi, E. L.; Amenitsch, H.; Brunet-Bruneau, A.; Bourgeois, A.; Sanchez, C. *Adv. Funct. Mater.* **2004**, *14*, 309–322.
(4) Lee, U. H.; Yang, J.-H.; Lee, H.-J.; Park, J.-Y.; Lee, K.-R.; Kwon, Y.-U. *J. Mater. Chem.* **2008**, *18*, 1881–1888.
(5) Ogawa, M. *J. Am. Chem. Soc.* **1994**, *116*, 7941–7942.
(6) Ogawa, M.; Igarashi, T.; Kuroda, K. *Bull. Chem. Soc. Jpn.* **1997**, *70*, 2833–2837.
(7) Petkov, N.; Mintova, S.; Jean, B.; Metzger, T. H.; Bein, T. *Chem. Mater.* **2003**, *15*, 2240–2246.
(8) Decher, G. *Science* **1997**, *277*, 1232–1237.
(9) Peterson, R. A.; Webster, E. T.; Niezyniecki, G. M.; Anderson, M. A.; Hill, C. G. *Sep. Sci. Technol.* **1995**, *30*, 1689–1709.
(10) Yang, H.; Kuperman, A.; Coombs, N.; Mamiche-Afara, S.; Ozin, G. A. *Nature* **1996**, *379*, 703–705.
(11) Schacht, S.; Huo, Q.; VoigtMartin, I. G.; Stucky, G. D.; Schuth, F. *Science* **1996**, *273*, 768–771.
(12) Yang, H.; Coombs, N.; Sokolov, I.; Ozin, G. A. *Nature* **1996**, *381*, 589–592.
(13) Aksay, I. A.; Trau, M.; Manne, S.; Honma, I.; Yao, N.; Zhou, L.; Fenter, P.; Eisenberger, P. M.; Gruner, S. M. *Science* **1996**, *273*, 892–898.
(14) Edler, K. J. *Aust. J. Chem.* **2005**, *58*, 627–643.
(15) Tolbert, S. H.; Schaffer, T. E.; Feng, J. L.; Hansma, P. K.; Stucky, G. D. *Chem. Mater.* **1997**, *9*, 1962–1967.
(16) Fernandez-Martin, C.; Edler, K. J.; Roser, S. J. *J. Mater. Chem.* **2008**, *18*, 1222–1231.

10.1021/cm802063m CCC: $40.75
Published on Web 03/03/2009

based on the spontaneous build-up of ordered structure, is more efficient, quickly forming films with a thickness range from nanometers to micrometers. However, most of the free-standing inorganic films are brittle, which limits their practical application.

Polymerizing silica has been found to act as a neutral polyelectrolyte during the formation of nanostructured silica−surfactant films;[17] thus, substituting the silica with a carbon polyelectrolyte also results in formation of a solid, ordered liquid crystalline phase at the air−water interface. Previously we have reported that mixing polyethylenimine (PEI) and cationic alkyltrimethylammonium bromide (CTAB) surfactant results in a solid film with well organized 2D hexagonal structure composed of cylindrical micelles aligned to the air−solution interface.[17] Vaknin also later reported a 2D hexagonal phase composed of closely packed cylindrical micelles aligned parallel to the interface, similar to that observed in inorganic−surfactant films, using mixtures of poly(diallyl-dimethylammonium chloride) and sodium dodecyl sulfate (SDS) at the air−water interface.[18] Compared to inorganic films, polyelectrolyte−surfactant films are much more flexible and robust, allowing them to be removed easily from the solution surface and resulting in free-standing films.[19] These films have the potential to act as a delivery system for hydrophobic compounds, such as hydrophobic drugs,[20] which could be released through film breakdown or slow diffusion out from the polymer−surfactant film. Here we have instead utilized them as templates for silica.

Surfactant−polyelectrolyte complexes have been known for quite a while to form highly ordered organic solids with mesomorphous structures.[21] Such complexes generally form because of the Coulombic interaction between the charged functional groups of the polyelectrolyte and an oppositely charged surfactant. Complexes of oppositely charged polyelectrolytes and surfactants were used in the presence of a silica source to prepare a series of mesoporous powders with different pore structures and morphology. Pantazis and Pomonis reported SBA-1 mesoporous silica particles templated by a poly(acrylic acid)−CTAB complex under acidic conditions, while addition of alkaline earths resulted in different morphologies.[22] Silicas synthesized using CTAB and poly(4-styrenesulfonate sodium) (PSS) were without ordered mesostructures.[23] In the work of Pantazis and Pomonis,[22] the pores were templated on the entire polymer−surfactant complex, not just the surfactant micelles, since the pore size varied with the size of the complex, controlled by the ionization degree of the polymer. Pang et al. also studied mesoporous silica templated by CTAB and two ionic polymers, the anionic sulfonated aromatic poly(ether ether ketone) (SPEEK) or cationic poly(allylamine hydrochloride) (PAACl).[24] Using the anionic polymer with CTAB produced bimodal pores, templated either on the CTAB micelles (∼2 nm) or the nanophase separated polymer particles (∼20−50 nm), while the cationic polymer used with CTAB produced unimodal pores (∼2−3 nm) with increasing disorder as the concentration of polymer increased. Highly ordered mesoporous materials constructed using mixtures of CTAB with poly(acrylic acid) having an integrated polymer−silica hybrid framework templated on the CTAB micelles were also reported by Kang et al.[25] However, these studies of mesoporous materials synthesized with polyelectrolyte−surfactant complexes are concerned with powders, and they lack long-range ordering of the mesostructure, regular morphology, or thermal stability. In this paper we present instead the use of polymer−surfactant complexes as co-templates for the spontaneous formation of thick robust films at the air−solution interface.

Free-standing nanostructured CTAB−PEI films at the air−water surface have now been extensively studied by our group;[19,26,27] however, using the CTAB−PEI complex in the presence of silicate precursors has not yet been reported. Here, we first report investigations of the robust dried CTAB−PEI films without silica, which retained mesostructural order to some extent after removal from the solution surface, followed by studies of the spontaneously formed silica films synthesized using these CTAB−PEI solutions in the presence of silica to form films at the air−water interface. All these films were removed from the surface to produce dried free-standing silica films. Most films displayed long-range 2D hexagonal mesostructures and retained their mesostructures even after the removal of template. Notably these films form at high pH, whereas previous work on film formation, including dip and spin coating as well as spontaneous growth of films at the solution surface, has required acidic solutions. Normally in alkaline solutions only precipitates are formed. These stronger, thicker mesoporous silica films have improved mechanical strength over thinner, brittle silica−surfactant only films and retain the polymer in the silica walls, providing a simple method of introducing polymer functionality into the pore walls. These advantages open up potential applications in a variety of fields such as catalysis, molecular separation, and drug delivery. To the best of our knowledge, this is the first report of a one step process to synthesize a mesoporous silica film with long-range order and high hydrothermal stability templated by the surfactant−polyelectrolyte complex at the air−water surface.

Experimental Section

Branched PEI (MW = 750 000 (denoted as LPEI); 2000 Da (denoted as SPEI)) as 50% weight solutions in water, cetyltrim-

(17) Edler, K. J.; Goldar, A.; Brennan, T.; Roser, S. J. *Chem. Commun.* **2003**, 1724–1725.
(18) Vaknin, D.; Dahlke, S.; Travesset, A.; Nizri, G.; Magdassi, S. *Phys. Rev. Lett.* **2004**, *93*, 218302–218306.
(19) O'Driscoll, B. M. D.; Milsom, E.; Fernandez-Martin, C.; White, L.; Roser, S. J.; Edler, K. J. *Macromolecules* **2005**, *38*, 8785–8794.
(20) O'Driscoll, B. M. D.; Hawley, A. M.; Edler, K. J. *J. Colloid Interface Sci.* **2008**, *317*, 585–592.
(21) Antonietti, M.; Conrad, J.; Thunemann, A. *Macromolecules* **1994**, *27*, 6007–6011.
(22) Pantazis, C. C.; Pomonis, P. J. *Chem. Mater.* **2003**, *15*, 2299–2300.
(23) Pantazis, C. C.; Katsoulidis, A. P.; Pomonis, P. J. *Chem. Mater.* **2006**, *18*, 149–154.
(24) Pang, J. B.; Na, H.; Lu, Y. F. *Microporous Mesoporous Mater.* **2005**, *86*, 89–95.
(25) Kang, Y. S.; Lee, H. I.; Zhang, Y.; Han, Y. J.; Yie, J. E.; Stucky, G. D.; Kim, J. M. *Chem. Commun.* **2004**, 1524–1525.
(26) O'Driscoll, B. M. D.; Fernandez-Martin, C.; Wilson, R. D.; Roser, S. J.; Edler, K. J. *J. Phys. Chem. B* **2006**, *110*, 5330–5336.
(27) O'Driscoll, B. M. D.; Fernandez-Martin, C.; Wilson, R. D.; Knott, J.; Roser, S. J.; Edler, K. J. *Langmuir* **2007**, *23*, 4589–4598.

ethylammonium bromide (CTAB), sodium hydroxide, ethylene glycol diglycidyl ether (EGDGE), and tetramethoxysilane (TMOS) were purchased from Sigma-Aldrich; all were used without further purification. Ultra-pure Milli-Q water (18.2 MΩ cm resistance) or D_2O (Sigma-Aldrich) was used as the solvent.

The concentration of CTAB was fixed at 0.037 M, which is above the critical micelle concentration (cmc) but below the sphere−rod micelle transition for the surfactant. The polymer concentration is given in grams of polymer per liter, and was varied from 10 g/L to 50 g/L. The concentration of cross-linker was changed from 0.02 M to 0.1 M. The concentration of TMOS varied from 0.0335 to 0.402 M. Usually no pH adjustment was made to the solution except where NaOH was added to SPEI solutions (as noted below), so the normal solution pH was 9−10, which increased to around 12 when NaOH was used.

To prepare the CTAB−PEI films without silica, a 0.074 M CTAB solution was mixed with an equal volume of polymer solution (to give a final concentration of 0.037 M CTAB), which was poured into a polystyrene dish over a piece of plastic mesh after a short period of stirring. Films grew at the air−solution interface and were removed from the solution surface by lifting the open plastic mesh from the bottom of the dish and dried in the air at room temperature. As we reported previously, to successfully remove film synthesized with low MW PEI (SPEI), EGDGE was added to the CTAB−SPEI mixture before pouring out, to cross-link the polymer.[27] Silica films were made by the same procedure by adding silicate precursor TMOS into the surfactant−polyelectrolyte mixture before pouring the solution into the dish to allow film formation to occur. To improve the mesostructure retention after removing the template, a silica film was exposed in a TMOS atmosphere in an oven at 40 °C for one day, and then the film was calcined under 600 °C for 6 h or else washed with ethanol to remove the surfactant template while retaining the polymer in the silicate walls.

Films were characterized during formation using Brewster angle microscopy (BAM) and neutron reflectivity, and small-angle X-ray scattering was used to characterize the subphase solutions as well as the recovered dried films. Thermogravimetric analysis (TGA) was used to characterize the amount of organic species in the dried silica films. The BAM images were collected using a NFT Nanoscope2 Brewster angle microscope. The SAXS results were collected on a PANalytical/Anton Paar SAXSess system with a PW 3830 generator. Neutron reflectivity was recorded on the SURF instrument at the ISIS Pulsed Neutron and Muon source, Rutherford Appleton Laboratories, Chilton, U.K. The incident angle used for the reflectivity experiment was 1.5°, with data being collected between 0.048 and 0.613 $Å^{-1}$ on D_2O at room temperature. The reflectometry profiles were modeled with the Motofit Program in Igor PRO platform (WaveMetrics).[28] TGA experiments were performed on a Perkin-Elmer TGA7 under nitrogen flow in the temperature range from 0 to 1000 °C at a heating rate of 5 °C/min.

Results

Dried Surfactant−Polyelectrolyte Films Removed from the Air/Water Surface. In our previous papers, surfactant−polyelectrolyte films formed at the air/water surface have been extensively studied in situ.[19,27] Films at the solution surface formed from low MW PEI (SPEI) are thin and contain a more highly ordered mesostructure than those formed from high MW PEI (LPEI).[19] The ordering, however, is maintained down to extremely low polymer and surfactant concentrations, even below the surfactant cmc.[29] Cross-linking causes little change in the mesostructure in in situ films but helps to freeze the metastable mesostructure and makes films strong enough to be removed from the solution surface.[27] Increasing the pH of the solution causes formation of thicker films and improves ordering in low MW films, while high MW films can lose some order, although this occurs only at high polymer concentrations.[27] Films are robust enough to be removed from the surface on an open mesh, as shown in Supporting Information Figure 1; the film is continuous, rubbery, and slightly tacky as a result of the hydrophilic nature of the polymer.

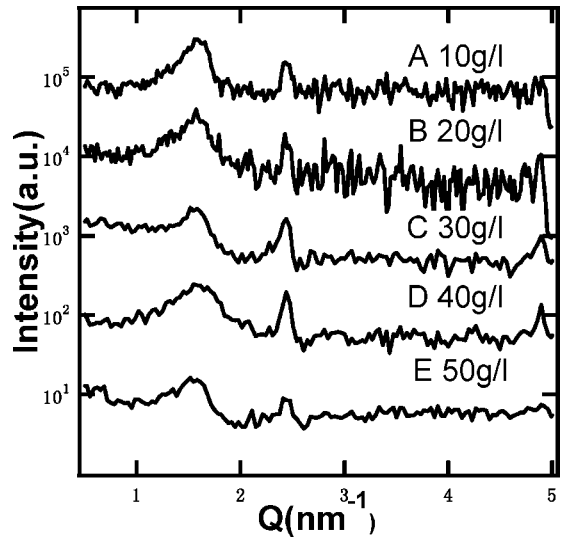

Figure 1. SAXS patterns of dried polymer films synthesized with (top to bottom) CTAB:10 g/L LPEI, CTAB:20 g/L LPEI, CTAB:30 g/L LPEI, CTAB:40 g/L LPEI, and CTAB:50 g/L LPEI. No cross-linker (EGDGE) was used to prepare these films.

SAXS patterns of the dried polymer films synthesized with CTAB and different concentrations of LPEI (from 10 g/L to 50 g/L), but without silica, are given in Figure 1. All of these patterns show a wide peak at 0.15 $Å^{-1}$, indicating that the mesostructure is retained but overall has relatively poor long-range order. The intensity and shape of the peak do not change with increasing LPEI concentration which shows that the solution concentration of LPEI makes little difference to the dried polymer film mesostructure. A second sharper peak at 0.24 $Å^{-1}$ is from excess crystalline CTAB, which is assumed to be formed on the film surface where droplets of the subphase have dried. Compared to grazing incidence diffraction and neutron reflectivity data from CTAB−LPEI films at the air/water surface, which also show partially ordered structures and broad diffraction peaks,[27] the dried films preserve their mesoscale structure during the drying process. The *d* spacing decreases from 5.4 nm for in situ films to 4.0 nm in dried films, which indicates shrinkage of the lattice spacing due to loss of water from the polymer hydrogel between micelles during the drying process.

Cross-linker plays an important role in preparing the dried CTAB−PEI films. By cross-linking the polymer, permanent

(28) Nelson, A. *J. Appl. Crystallogr.* **2006**, *39*, 273–276.

(29) Comas-Rojas, H.; Aluicio-Sarduy, E.; Rodríguez-Calvo, S.; Pérez-Gramatges, A.; Roser, S. J.; Edler, K. J. *Soft Matter* **2007**, *2*, 747–753.

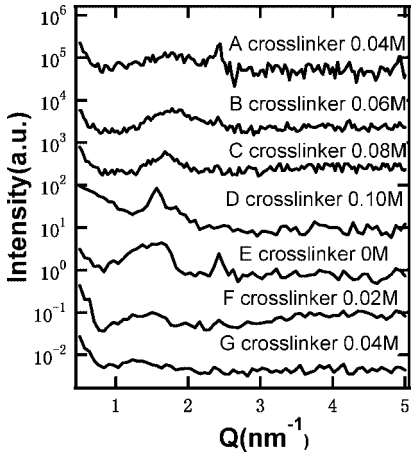

Figure 2. SAXS patterns of dried polymer films synthesized using cross-linker at pH 12 for concentrations of 0.037 M CTAB:15 g/L SPEI with (top to bottom, A−D) 0.04 M, 0.06 M, 0.08 M, and 0.1 M EGDGE and for solution concentrations of 0.037 M CTAB:30 g/L LPEI at pH 9 for concentrations of (E−G) 0 M, 0.02 M, and 0.04 M EGDGE.

covalent bonds are formed between adjacent polymer strands, creating a stronger and more permanent linkage than the hydrogen bonding and polymer entanglement which holds the films together in the absence of cross-linker. Ethylene glycol diglycidyl ether (EGDGE) is a commonly used cross-linking agent for PEI, and the reaction occurs at room temperature in ambient conditions.[30] In our observations, cross-linking in the films proceeds much faster than in the subphase solutions, as a result of the higher concentration at the interface. This allows cross-linked films to be removed from the liquid surface, since subphase gelation by the cross-linker does not occur for several hours after the cross-linking of the film is complete.

However, for films synthesized with LPEI (Figure 2E−G), the first diffraction peak in SAXS patterns becomes less distinct as the concentration of EGDGE increases, which indicates that the cross-linking reaction reduces the ordering of the dried films synthesized with LPEI. In contrast, for SPEI without cross-linker, all the films were either difficult to remove intact from the air/water interface or display a disordered structure after drying. Higher pH is known to improve film ordering on the solution surface and increases film thickness, because the charge on PEI decreases at higher pH, and thus the polymer can interact more effectively with CTAB micelles through ion−dipole interactions.[30] Thus to improve the structure of the dried SPEI films, the pH was increased to 12 by adding sodium hydroxide to the CTAB−SPEI system. Similarly the effect of cross-linker has also been studied, since cross-linked films are stronger than those without cross-linking and are more easily removed from the solution surface without breaking. Cross-linking also was found to improve the mesostructure, as shown in Figure 2A−D. The first peak around 0.16 Å^{-1} becomes more distinct with increasing cross-linker concentration which shows that cross-linker helps to improve the structural ordering in the SPEI films.

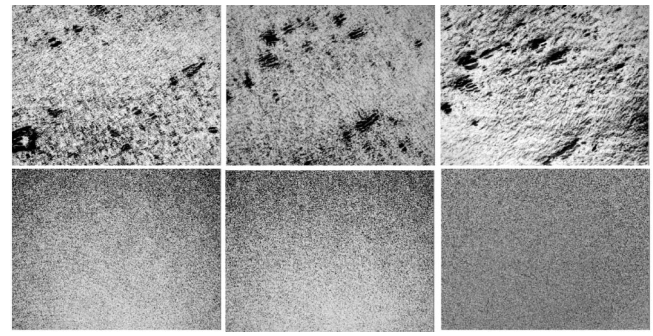

Figure 3. BAM pictures of silica films grown at the air−water interface. At the top are films synthesized with CTAB:LPEI at (left to right) 0 min, 10 min, and 20 min, and at the bottom are films synthesized with CTAB:SPEI at (left to right) 0 min, 30 min, and 5 h, respectively. The images are all 340 μm along the bottom edge.

Silica Films Synthesized with Surfactant−Polyelectrolyte Complexes at the Air/Water Surface. Silica films synthesized with surfactant at the air/water interface have been previously extensively studied by our group.[16,31−33] Here, silica films have instead been synthesized using the surfactant−polyelectrolyte complex (see Supporting Information Figure 2) rather than the simple surfactant templates used in the previous studies. Free-standing solid films form readily from the mixed PEI/CTAB/TMOS solutions and can be clearly seen at the air/water interface. Films synthesized with LPEI develop rapidly and are clear, transparent, and initially smooth but develop wrinkles upon aging. The film formation process for films synthesized with SPEI, in contrast, is relatively slow, the film is white and smooth, and precipitation in the subphase solution could also be seen.

BAM pictures of silica films, shown in Figure 3, were taken immediately after the mixture of the silicate precursor and surfactant−polymer solution was poured into a plastic dish and at intervals until film formation had occurred. The surfaces of silica−CTAB−LEPI solutions were mobile during the first 10 min and became still thereafter, indicating the formation of more continuous, solid, and less mobile films. The films become thick and rough at about 20 min, and the images look similar to those of CTAB−silica films prepared without PEI.[31−33] Silica films synthesized with CTAB−SPEI initially are similar to those with CTAB−LPEI but keep growing for longer, and after 5 h the film was much thicker and smoother than the CTAB−LPEI film. The overall times for formation of silica films synthesized with SPEI were much longer than the times for films synthesized with LPEI, but films synthesized with SPEI were much smoother on the micrometer length scale than films synthesized with LPEI.

Neutron reflectivity patterns for the silica films synthesized with CTAB−LPEI are shown in Figure 4. In general the LPEI films show little evidence of long-range mesostructural

(30) Kokufuta, E.; Suzuki, H.; Yoshida, R.; Yamada, K.; Hirata, M.; Kaneko, F. *Langmuir* **1998**, *14*, 788–795.
(31) Edler, K. J.; Goldar, A.; Hughes, A. V.; Roser, S. J.; Mann, S. *Microporous Mesoporous Mater.* **2001**, *44*, 661–670.
(32) Fernandez-Martin, C.; Roser, S. J.; Edler, K. J. *Langmuir* **2004**, *20*, 10679–10684.
(33) Edler, K. J.; Brennan, T.; Roser, S. J.; Mann, S.; Richardson, R. M. *Microporous Mesoporous Mater.* **2003**, *62*, 165–175.

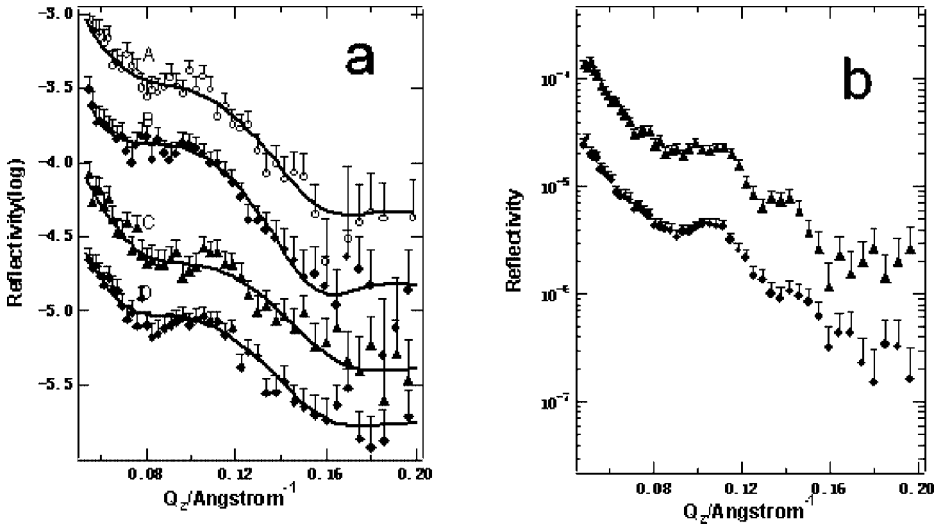

Figure 4. Neutron reflectivity patterns of silica films growing at the air−water interface synthesized with different concentrations of TMOS and LPEI. (a) Films without long-range liquid crystalline order (A, B are the 30 g/L LPEI:0.335 M TMOS film at 15 min and 45 min, respectively; C, 30 g/L LPEI:0.167 M TMOS film at 45 min; D, 20 g/L LPEI:0.167 M TMOS film at 45 min). A line of best fit to the original data is also shown (see text). (b) Films from 40 g/L LPEI:0.134 M TMOS at 15 min (top) and 45 min (bottom). CTAB concentration was constant at 0.037 M.

ordering as they grow. Figure 4a shows films whose neutron reflectivity patterns have no distinct diffraction peaks, with lines showing the best fit to a layer model described in Supporting Information Table 1. The scattering length density (SLD) data from the fit suggests that these silica films synthesized with CTAB:LPEI contain ∼4 layers; the first layer is a single CTAB monolayer lying close to the surface with a disordered silicate/PEI layer beneath. The SLD of the third layer decreases because of the CTAB micelles incorporated into this layer, but this layer also contains PEI and silica. The SLD of the last layer is almost equal to the SLD of the sub-phase of the solution. As the film continues to grow at the air/water surface, the SLD of second layer increases as a result of the condensation of TMOS, and the SLD of the last layer decreases to around 2×10^{-6} Å^{-2}, suggesting there is another layer of micelle-containing adsorbed material present. The film layer structure does not seem to change much with the variation of LPEI and TMOS concentration. In Figure 4b an in situ LPEI/CTAB/silica film with two broad diffraction peaks was observed, giving a spacing between adjacent repeat units of 65 Å, and again the structure does not change during the film growth process.

Neutron reflectivity patterns for the silica films synthesized with TMOS:SPEI shown in Figure 5 show a greater range of mesostructural order. Figure 5a is a film synthesized with 0.037 M CTAB:20 g/L SPEI:0.134 M TMOS:0.04 M EGDGE where no distinct peaks were observed. Fitting results, also in Supporting Information Table 1, shows this film has a similar layer structure to films synthesized with LPEI. Figure 5b is a film synthesized with the same PEI/CTAB/EGDGE concentrations but more TMOS. Here the intensity of the diffraction peaks decreased with time, which is normal for PEI/CTAB films without silica, synthesized at a low concentration of SPEI.[27] The disappearing peak is due to the redistribution or reorientation of the inorganic−polymer−surfactant aggregates into thinner layers with time, and these thinner layers do not give rise to diffraction peaks, only fringes in the reflectivity. Figure 5c−f shows films with several distinct diffraction peaks. For all those films, two distinct peaks at about 0.12 Å^{-1} and 0.14 Å^{-1} (corresponding to *d*-spacings of 52.3 Å and 44.8 Å) were observed at the beginning of the reaction, which can be indexed to a cubic phase, although further work is needed to unambiguously confirm its structure. The position of these two peaks does not change as the SPEI concentration is varied. However, the intensity of the first peak decreases, and that of the second peak increases with time, which indicates that the silica film structure is changing. The film synthesized with EGDGE changed structure faster, with the transition occurring at about 1 h after mixing, while the film synthesized without EGDGE underwent a similar transition at about 2 h after mixing. Given that the position of the second peak which increases in intensity in the neutron reflectivity is similar to that of the first diffraction peak in SAXS data of dry films which have a 2D hexagonal mesostructure, as shown in Figure 7 (below), we deduce that films at the air/water surface change from an initial cubic structure to a final 2D hexagonal structure while still on the solution surface; thus, the structural transition is not caused by the drying of the film after it is removed from the surface but by the continuing silica condensation and surface dehydration while the film is still on the solution surface. Comparing parts c and d and parts e and f of Figure 5, we can see that the addition of cross-linker speeds up the formation of films but has little effect on the silica film structure.

Dried Silica Films Synthesized with Surfactant−Polyelectrolyte Complexes. Silica films templated by surfactant and both types of PEI mentioned above are robust to removal from the air/water interface to form free-standing films (Figure 6). The films synthesized with LPEI remain continuous without cracking after drying; however, films synthesized with SPEI are white and smooth and crack near the mesh strands. The film morphology is still retained even after calcination, suggesting the polymer in the template improves the film strength, possibly by increasing film thickness over surfactant-only templated silica films, which are extremely fragile and tend to fracture into powders after calcination.

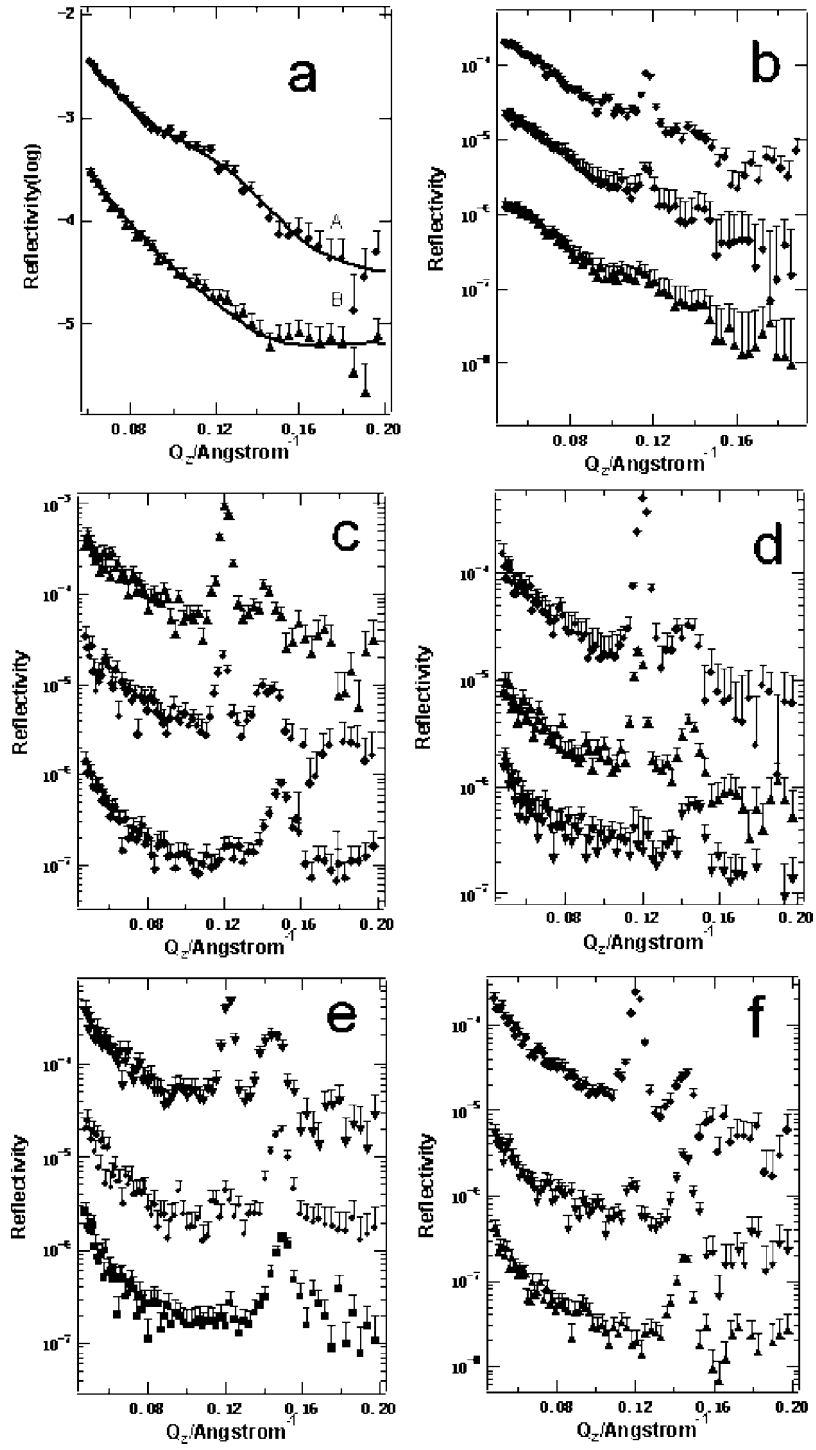

Figure 5. Neutron reflectivity patterns of silica films grown at the air−water surface synthesized with different concentrations of TMOS and SPEI. (a) 20 g/L SPEI:0.134 M TMOS:0.04 M EGDGE, a best fit line to the data is also shown. (b) 20 g/L SPEI:0.084 M TMOS:0.4 M EGDGE film at 15 min to 1 h (from top to bottom). (c) 30 g/L SPEI:0.084 M TMOS film at 15 min to 2 h (from top to bottom). (d) 30 g/L SPEI:0.084 M TMOS:0.04 M EGDGE at 30 min to 1 h (from top to bottom). (e) 40 g/L SPEI:0.084 M TMOS at 30 min to 2 h (from top to bottom). (f) is 40 g/L SPEI:0.084 M TMOS:0.04 M EGDGE at 30 min to 1 h (from top to bottom).

The SAXS patterns of dried films synthesized with CTAB−LPEI are shown in Figure 7, and the peak position and *d*-spacings are listed in Supporting Information Table 2. The SAXS patterns are shown for all samples where films were observed (see phase diagram in Figure 9 below). Figure 7a (A−E,G,H) shows one broad peak around 0.14 $Å^{-1}$, indicating a low degree of long-range order, and the peak at 0.24 $Å^{-1}$ is from excess crystalline CTAB. However, the

Figure 6. Picture of dried silica films synthesized with (left) CTAB:LPEI and (right) CTAB:SPEI.

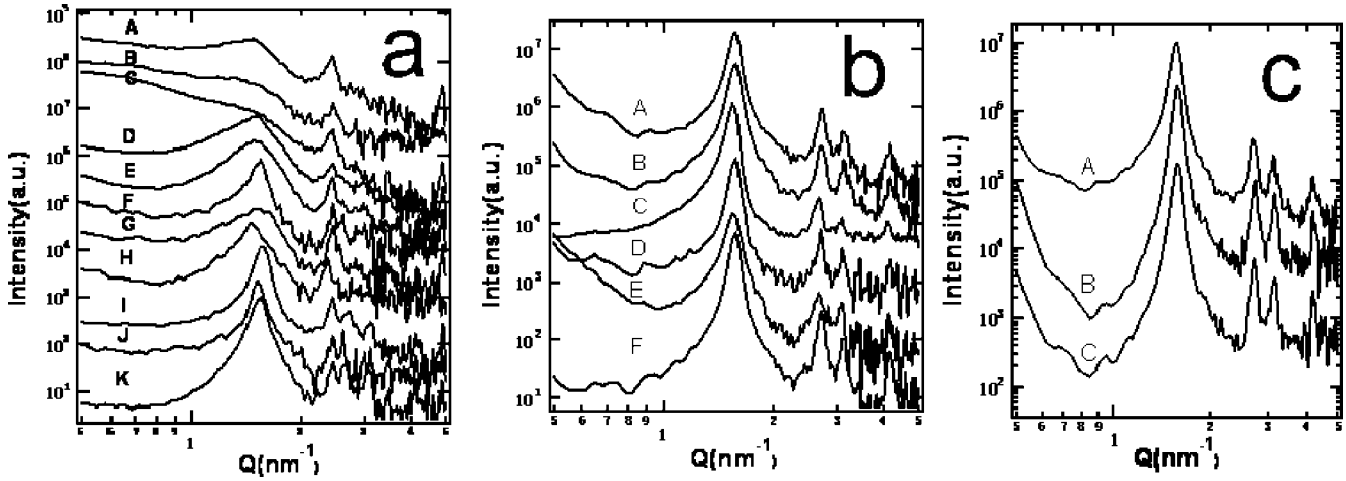

Figure 7. (a) SAXS patterns of dry silica films synthesized with CTAB−LPEI. A (30 g/L LPEI:0.168 M TMOS), B (10 g/L LPEI:0.084 M TMOS), C (20 g/L LPEI:0.1675 M TMOS), D (10 g/L LPEI:0.034 M TMOS), E (20 g/L LPEI:0.084 M TMOS), F (40 g/L LPEI:0.168 M TMOS), G (30 g/L LPEI:0.034 M TMOS), H (20 g/L LPEI:0.034 M TMOS), I (40 g/L LPEI:0.084 M TMOS), J (40 g/L LPEI:0.034 M TMOS), K (30 g/L LPEI:0.084 M TMOS). CTAB concentration is constant at 0.037 M. (b) SAXS patterns of dry silica films synthesized with CTAB:SPEI. A (30 g/L SPEI:0.168 M TMOS), B (30 g/L SPEI:0.084 M TMOS), C (40 g/L SPEI:0.084 M TMOS), D (20 g/L SPEI:0.034 M TMOS), E (30 g/L SPEI:0.034 M TMOS), F (20 g/L SPEI:0.084 M TMOS) at a CTAB concentration of 0.037 M and cross-linker concentration of 0.04 M. (c) SAXS patterns of dry silica films synthesized with different concentrations of cross-linker EGDGE: A (0.04 M), B (0.06 M), and C (0.02 M) for a CTAB concentration of 0.037 M, 30 g/L SPEI, and 0.1 M TMOS.

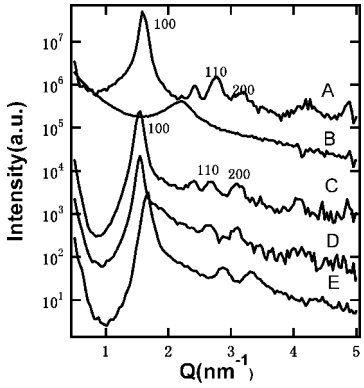

Figure 8. SAXS pattern of as-synthesized (A) and calcined (B) silica film synthesized with CTAB:30 g/L SPEI. C is as-synthesized film after exposure to TMOS vapor for a day. D and E are SAXS patterns of C films with the surfactant template removed by calcination and washing by ethanol, respectively.

SAXS patterns of samples of Figure 7a (F,I−K) show three low angle Bragg peaks indexed as (100), (110), and (200), corresponding to the long-range ordered 2D-hexagonal phase, with *d*-spacings between 4.59 nm and 4.79 nm. Variation of the concentrations of LPEI and TMOS does not significantly alter the peak positions. Compared with neutron reflectivity data in Figure 4, the drying process appears to improve the ordering of the micelles within these films, possibly since film shrinkage forces the charged micelles closer together, so electrostatic interactions between adjacent micelles force greater ordering in the films.

The SAXS pattern of silica dried films synthesized with CTAB:SPEI are shown in Figure 7b and the peak position and *d*-spacings are given in Supporting Information Table 3. All of these samples show three low angle Bragg peaks indexed as (100), (110), and (200), corresponding to long-range ordering in a 2D-hexagonal structure, with *d*-spacing around 4.6 nm. Again, variation of SPEI and TMOS concentrations do not have a great effect on the film structure. The effect of cross-linker has also been studied, as shown in Figure 7c. The concentration of cross-linker has been changed from 0.02 to 0.06 M when CTAB is 0.037 M, SPEI is 30 g/L, and TMOS is 0.1 M. The peak positions are unchanged, suggesting cross-linker also has little influence on the final structure of the silica film synthesized with CTAB−SPEI, which corresponds well with the neutron reflectivity data above.

The most elementary proof for the composite nature of the sample is its thermal weight-loss behavior, and TGA patterns of silica films synthesized with CTAB:30 g/L LPEI or CTAB:30 g/L SPEI are given in Supporting Information Figure 3. These indicate that the films have a composition of about 35% silica and 45% organics for films synthesized with LPEI, and 25% silica and 60% organics for films synthesized with SPEI, respectively. These two samples showed a similar decomposition pattern of three degradation weight-loss steps. The first drop in weight (up to 150 °C) is due to water loss. The next step at 150 °C−250 °C is the range of polymer and surfactant loss by combustion. Weight loss at temperatures between 250 °C and 500 °C is due to the further condensation of silicate. Silica films synthesized with LPEI contain more inorganic material than films synthesized with SPEI.

The organic material in the films was removed either by calcination or by washing with ethanol. A sample calcined in air at 600 °C for 6 h is shown in Figure 8 B. The first peak becomes less distinct, but the higher orders disappear and the peak position shifts to higher Q value, suggesting a decrease of the long-range order and unit cell spacing. However, when samples were exposed to TMOS vapor for 24 h before calcination, the three distinct peaks in Figure 8 D shows that the 2D hexagonal pore ordering is retained well after calcination. This indicates the high thermal stability of these films, although the *d*-spacing is still decreased, to 4.3 nm. Samples where surfactant removal was carried out by washing in ethanol after exposure to TMOS vapor for

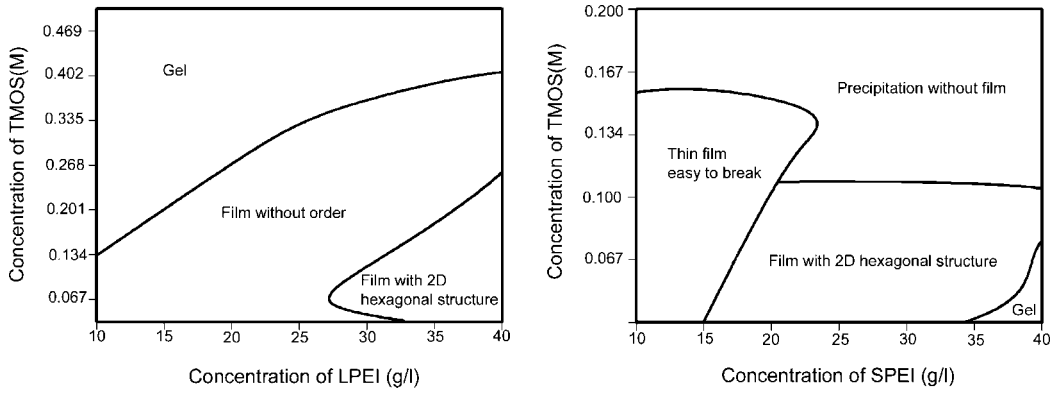

Figure 9. Phase diagram of CTAB−PEI−TMOS film forming system. (CTAB−LPEI−TMOS, left, and CTAB−SPEI−TMOS, right).

one day are also shown in Figure 8. In these films, not only is the 2D hexagonal pore order well retained, but also the *d*-spacing is constant, indicating no shrinkage of unit cell during template removal.

On the basis of these experimental results, both from neutron reflectivity measurements of film growth at the air/water surface and from SAXS studies of the dried free-standing films, the phase diagrams of the CTAB/TMOS/LPEI and CTAB/TMOS/SPEI film forming systems are presented in Figure 9, in which the concentration regions where different film phases exist are depicted. In the CTAB/TMOS/LPEI system, the region for gel formation (where no films form, as the entire solution gels), ordered film, and disordered films have been examined. Silica gelation was observed at high TMOS concentration and low LPEI concentration. With an increase of LPEI concentration and decrease of TMOS concentration, films formed and the film structure became more ordered: neutron reflectivity data on the films at the air/water surface shows some ordering at low TMOS concentration and high LPEI concentration. When taken off the surface and dried, these films present a highly ordered 2D hexagonal structure, indicating that the drying process improved the ordering of the film. However, for intermediate concentrations where the neutron reflectivity measurements showed no ordering of the film on the solution surface, dried films also contained no long-range mesostructural ordering.

In the CTAB/TMOS/SPEI system, 0.04 M EGDGE was used in all these preparations. The film at the air−water surface is too thin to be removed from the surface at low concentrations of TMOS and low concentrations of SPEI, but with an increase of concentration of SPEI, the system separated into two phases; precipitation of a composite without film formation was found at high concentration of TMOS, and this precipitated powder also shows ordered 2D hexagonal mesostructures. At low concentration of TMOS, films at the air/water interface present initially a cubic phase and change into 2D hexagonal with time, and this ordered 2D hexagonal structure was retained when the films were dried. Again the regions where neutron reflectivity indicated ordered film formation at the solution surface correspond with the concentrations where films that retained order after drying could be recovered from the solution surface. Gelation of the entire solution was also observed, at even higher concentrations of SPEI and lower TMOS.

Discussion

Previously, polymer−surfactant films at the air/water surface have been extensively studied in our group, and we have suggested a possible mechanism for the formation of the polymer films at the air/water interface.[27] Upon mixing the solutions of cationic surfactant and polyethylenimine, there is an association in the solution forming aggregates with the micelles loosely trapped by polyelectrolyte chains. Hydrophobicity, as the major driving force, will drive the aggregates from solution to assemble at the air/water surface, resulting in the formation of films.[27] Evaporation causes the dehydration of the upper layers of the film and, thus, promotes the ordering of the film at the interface and helps assist further aggregation below it. Ordered films are therefore found over the entire concentration range where stable films are observed to form, even at very low polymer concentrations, and surfactant concentrations below the cmc for sufficiently high molecular weight (and thus hydrophobic) polymers.[29] For low molecular weight polymers where the polymer itself is more hydrophilic, unstable initially ordered films are observed to lose order with time by thinning, if there is insufficient material arriving at the interface to completely cover that interface with a substantial mesostructured layer.[27]

Using cross-linker in the reaction solution, polymer films synthesized with SPEI were able to be taken off of the surface and dried, and the dried films synthesized both with LPEI and with SPEI are shown here to preserve the nanoscale structure observed at the solution surface in our previous work. The cross-linker (EGDGE) has a great effect on the structural ordering of the dried films. Cross-linking caused disordering in the films synthesized with LPEI but enhances the ordering of the films synthesized with SPEI. EGDGE contains two epoxides that are susceptible to nucleophilic addition reactions involving the imine groups on the polymer. Our cross-linking results suggest that there is an optimum polymer length for ordered mesostructured film formation. In the case of the hyper-branched LPEI, it is already longer than the optimal length for mesostructural ordering, so increasing the concentration of EGDGE will not only decrease the number of primary amine groups of the polymer, decreasing the dipole interaction between the polymer and surfactant micelles, but also distort the PEI chain, which induces disorder in the arrangement of the surfactant micelles.

Scheme 1. Proposed Mechanism of the Formation of Silica Films Templated by CTAB/PEI Complexes

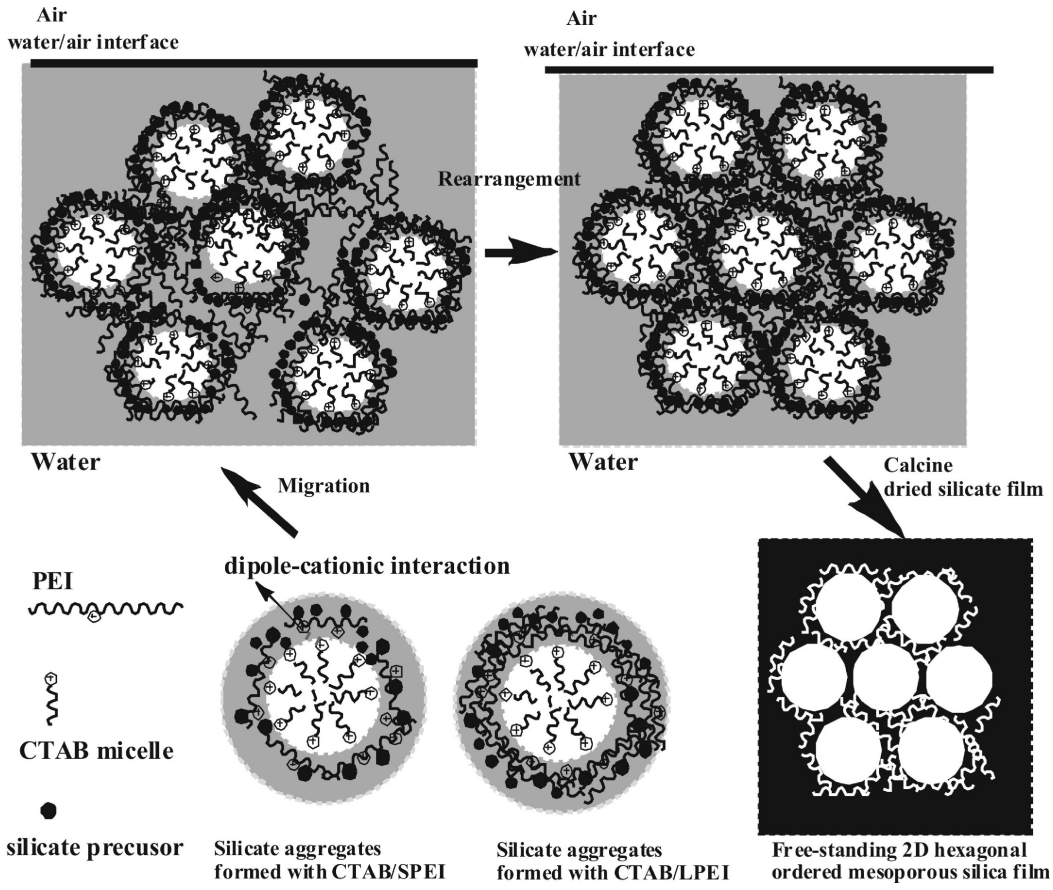

For the SPEI, the polymer is shorter than the optimum polymer length for film formation, so in this case increasing the concentration of the EGDGE will bridge between SPEI chains and bring the cross-linked polymer closer to the optimum length, helping to improve both film thickness and also mesostructural ordering.

Considering the above, we suggest a mechanistic scheme for the formation of silica films synthesized using the surfactant−polyelectrolyte complex at the air/water interface, by adding TMOS to the CTAB/PEI film forming solutions discussed in the above two paragraphs, shown in Scheme 1. In the pH range used for these experiments (between 9 to 12), PEI has a small net positive charge (∼3%), but the dominant interaction between the polymer and the surfactant is a dipole−cationic interaction, where the dipoles on the polymer amine groups interact with the charged CTAB quaternary ammonium group.[19] Thus the polymer chains surround the CTAB micelles in solution in a loose hydrogel but do not tightly bind to the micelle;[19] however, this loose binding sufficiently decreases the hydrophilicity of the polymer−surfactant complex that it becomes hydrophobic and migrates to the air−solution interface.[27] Silicate species are negatively charged under basic conditions, so they are electrostatically attracted to the cationic surfactant upon the mixture with the surfactant−polymer solution. There is also a strong interaction between the uncharged amine groups on the polymer with the negatively charged silica species; similar interactions are seen between silica anions and amines in the proteins responsible for biosilicification.[34]

The silica therefore infiltrates the surfactant−polymer complex, interacting both with the nitrogens in the polyelectrolyte chains and directly with the CTAB micelles. The collective electrostatic interactions and the dipole−cation interaction allow coassembly resulting in the homogeneous dispersion of the polymer and silicate species around the CTAB micelles. The interaction with silica does not affect the increasing hydrophobicity of the CTAB−PEI complex as long as the relative amount of silica is low, and this hydrophobicity as the main driving force, makes the CTAB−PEI−silicate complex migrate to the air/water interface. Where silica concentrations are high and the polymer molecular weight is low, precipitation instead of film formation is observed (Figure 9), since the silica can completely coat micelles and polymer, preventing polymer bridging between micelles. This bridging, which allows larger but still soluble hydrophobic aggregates to form and migrate to the interface, is essential for film formation to occur. The composite species formed in the subphase accumulate at the interface and continue to rearrange into a more ordered phase as the surface layers dehydrate, a process which continues as long as the film is not too viscous. Some films initially display a cubic structure and change into a 2D hexagonal phase with time, probably due to the micellar packing constraints,

(34) Cha, J. N.; Shimizu, K.; Zhou, Y.; Christiansen, S. C.; Chmelka, B. F.; Stucky, G. D.; Morse, D. E. *Proc. Natl. Acad. Sci. U.S.A.* **1999**, *96*, 361–365.
(35) Brennan, T.; Hughes, A. V.; Roser, S. J.; Mann, S.; Edler, K. J. *Langmuir* **2002**, *18*, 9838–9844.

specifically the headgroup area which is reduced as continuing silica condensation causes the structure to become more densely packed with time, increasing the local concentrations of silica around the surfactant headgroups and screening charge between adjacent headgroups more efficiently.

Silica films synthesized with LPEI form very rapidly with relatively low internal ordering. In this experiment, the PEI concentration is 30 g/L (the concentration of monomer units of polymer is 1.395 M, about 38 times of the concentration of the surfactant), and the polymer is long enough to completely wrap around the micelles. The long polymer chains are also able to bind several micelles and so span the region between micelles, filling this region more densely than in the case of SPEI. Thus in the LPEI/CTAB solutions, silicate species are less able to contact with the cationic surfactant directly, and no distinct silicate precipitation was seen in the solution. Because of the higher hydrophobicity of the LPEI, the migration of the aggregates to the surface is promoted, which results in a rapid phase separation and formation of the film. Phase separation and mesophase ordering within the film is competitive.[27] For high MW PEI the ordered structures take some time to form and ordering improves with time; thus, fast phase separation limits the self-ordering process of the micelles. Also, the higher viscosity of the LPEI−CTAB layer, due to the high polymer MW, prevents rearrangement of the mesostructure into a more ordered form. On the contrary, for silica films synthesized with SPEI, the film takes a longer time to form and has a highly ordered structure. The shorter PEI polymer is barely long enough to span the gap between two micelles, given the measured *d*-spacings from the films, so each polymer binds to at most two micelles, leading to a lower density hydrogel between and around the micelles. The negatively charged silicate species will interact both with the nitrogen containing polymer and directly with the cationic surfactant, where this electrostatic interaction results in precipitation of composite silicate species in the solution. We have investigated the precipitate, and it also has a 2D hexagonally ordered mesostructure. Because SPEI polymer chains are less hydrophobic and bind fewer micelles, the migration of aggregates to the surface is slower; thus, the phase separation to form the films takes a long time, and as a result of the low polymer molecular weight, the film itself is less viscous and contains less silica, which enables the ordering process, allowing the formation of highly ordered films. The addition of cross-linker does not change the silica film structure, as the cross-linking reaction occurs in tandem with the film formation and silica condensation processes. Essentially the cross-linking process makes short PEI longer and more hydrophobic, which speeds up the formation of films.

The addition of silica to PEI/CTAB solutions reduces the concentration range over which ordered films are observed to form at the air−solution interface but also stabilizes and thickens nonordered films. Such nonordered films are observed in the CTAB/PEI only phase diagram but are unstable and cannot be removed from the interface where they formed.[27,29] Similarly the presence of PEI in these silica−surfactant−polymer films reduces the region of concentration over which ordering is observed compared to films formed from acidic silica−surfactant solutions (with no polymer)[35] but allows film formation to occur at high pH where normally only precipitates are found. The addition of polymer results in greatly enhanced film thickness and thus improved thermal stability and the retention of film geometry after template removal which is seldom seen in silica surfactant-only films.

Conclusion

In this paper, solid CTAB/PEI films were removed from the air/water surface, and the nanostructure was shown to be retained in these polymer−surfactant films after drying. The extent of structural ordering was affected by the concentration of cross-linker but depends mainly on the molecular weight of the polymer. High molecular weight polymers form less ordered but thicker films, while low molecular weight polymers form more ordered films which require use of a cross-linker to make them thick enough to remove from the interface.

When TMOS is added to CTAB/PEI solutions, the CTAB/PEI/TMOS system presents different phases. Depending on concentration, the complexes will form amorphous gels or mesostructured precipitates or films. Some of the CTAB/PEI/silicate films had few or no ordered repeat layers when they formed in situ at the solution surface and thus result in disordered films when they are dried. However, at the air/water interface, most films show cubic phase ordering at the beginning of the film formation process and transform into a 2D hexagonal phase with time. This 2D hexagonal structure was retained when the films were dried. These silica films are strong and resist cracking, particularly for LPEI and have a high thermal stability since the ordered structure is maintained even after the removal of the template, which suggests potential applications in a variety of practical applications, such as membrane catalysis and molecular sieving where robust silica membranes are required.

The mechanism for the formation of this silica film templated by CTAB/PEI at the air/water interface has been proposed. The electrostatic interactions between the silicate species and CTAB/PEI as well as the dipole−cationic interaction between CTAB and PEI allow their co-assembly and result in the homogeneous dispersion of the polymer and silicate species around CTAB micelles. The binding of surfactant and polymer (either with or without silica) makes the complex increasingly hydrophobic, so it moves to the solution surface. Migration to the interface and rearrangement of these CTAB/PEI/silicate complexes at the solution surface results in films with highly ordered mesoscale structures.

Finally, an important implication of this work is that it is possible to balance the interaction between the surfactant, polymer, and silica precursor to achieve efficient co-assembly into a highly ordered mesostructured material. This work provides not only a straightforward way to introduce a polymer as part of the inorganic wall structure to make it more robust and mechanically strong but also incorporates organic species into the silicate wall. This raises the potential of using polymers to impart further chemical functionality to the pore walls of the silicate which could allow binding of specific species in the pores or allow synergistic interac-

tions between organic functionality from the polymer and inorganic species in the walls for catalysis. This is the first report of the synthesis of inorganic ordered mesoporous films templated by surfactant−polyelectrolyte complexes at the air/water interface. By altering the polyelectrolyte, surfactant, or inorganic precursor, a wide range of free-standing organic−inorganic hybrid films could be generated at the air/water interface.

Acknowledgment. We wish to thank the beamline scientists Dr. Arwel Hughes and Dr. Phil Taylor on SURF at ISIS, RAL, James Holdaway and Robert Barker for assistance with collecting the SURF data, and Dr. Steve Roser for allowing use of the Brewster angle microscope. We also thank the University of Bath and the ORSAS scheme for funding.

Supporting Information Available: Additional pictures, fitting results for the neutron reflectivity patterns, peak positions and *d*-spacings measured from the SAXS patterns, and TGA (PDF). This material is available free of charge via the Internet at http://pubs.acs.org.

CM802063M